Lithos 376–377 (2020) 105755

Contents lists available at ScienceDirect

Lithos

journal homepage: www.elsevier.com/locate/lithos

Research Article

U-Pb systematics in volcanic and plutonic rocks of the Krokskogen area: Resolving a 40 million years long evolution in the Oslo Rift

Fernando Corfu *, Bjørn Tore Larsen

Department of Geosciences and CEED, University of Oslo, P.O. Box 1047 Blindern, N-0316 Oslo, Norway

ARTICLE INFO

Article history:
Received 12 June 2020
Received in revised form 19 August 2020
Accepted 22 August 2020
Available online 27 August 2020

Keywords:
U-Pb
Zircon
Baddeleyite
Oslo Rift
Rhomb porphyry
Volcanic complex

ABSTRACT

The development of the Oslo Rift started in the latest Carboniferous in the northern foreland of the Variscan Orogen. The initial, intensive, and mainly mafic magmatism at around 300 Ma, was followed by a period of some 40 m.y. of mafic and felsic volcanic and plutonic activity. The present study applied U-Pb in zircon on rocks of the Krokskogen area northwest of Oslo to resolve in greater detail the sequence of events in this evolution. A major challenge, however, has been the absence or paucity of zircon, and their low quality for dating, in some of the important units, especially the alkalic (latitic) rhomb porphyries. The earliest rhomb porphyry flow RP1 yields an age of 299.7 ± 0.4 Ma. It was thus coeval with the earliest basaltic and alkalic eruptions in the southern part of the Oslo Graben. Flows RP6 and RP7 yield overlapping ages of 285.5 ± 0.8 and 284.9 ± 0.5 Ma, and RP11 is 280.2 ± 0.5 Ma. The Bærum, Oppkuven and Heggelia caldera volcanoes, and the Slottet kjelsåsite pluton developed at 276.7 to 275.9 Ma while the Øyangen caldera is somewhat younger at 273–272 Ma. A kjelsåsite stock has an age of 265.4 ± 0.6 Ma, predating the 262.3 ± 0.5 Ma Blindern rhomb porphyry-like dyke, which is among the youngest magmatic expressions in the rift. The new data stress the importance of the magmatic burst at around 300 Ma, possibly plume related, along the entire Oslo Rift, and sharpens our understanding of the timing of the subsequent protracted sequence of magmatic events reflecting continuous heating and stress in the lithosphere, likely broadly controlled by processes accompanying the closing of Pangea.

1. Introduction

The Oslo Rift developed in the latest Carboniferous and Permian in the foreland of the Variscan Orogen by lithospheric stretching, sedimentation and basaltic to felsic magmatism (Larsen et al., 2008; Olaussen et al., 1994). The activity persisted for about 40 to 50 m.y. (Sundvoll et al., 1990). The initial phases were synchronous with the late tectonic stages in the Variscan Orogen farther south, itself a product of the processes that led to the assembly of Pangea. It is probable that there were causal links between the processes associated with the supercontinent assembly, the Variscan Orogeny and rifting plus magmatism in the Variscan foreland, but other factors were likely also of fundamental importance in building the Oslo Rift. Such as the role of a mantle plume, which has been suggested based on the nature of some of the magmatic suites (e.g. Neumann, 2019), the intensity and regional extent of the initial pulse of magmatism, and the restored position of the region vertically above the edge of the African Large Low Shear Velocity Province (Torsvik et al., 2008). Questions related to the genesis of the Oslo Rift have been addressed by diverse geological and geophysical studies for more than a century, revealing very special phenomena in terms of unique rock and mineral types, volcanic processes, structures, and lithospheric geometries. The timing of the sequence of events has been studied extensively, especially by Rb-Sr and Sm-Nd techniques in the 70's and 80's (e.g. Sundvoll et al., 1990), documenting regional age patterns and the relative longevity of the rifting and magmatic processes. Modern ID-TIMS U-Pb geochronology offers the means to refine the existing temporal framework by resolving more in detail the sequences of events, and correcting biases introduced in some of the Rb-Sr data by the widespread alteration that overprinted the rocks. The approach with U-Pb, however, is not without challenges, especially due to the difficulty of finding suitable zircon or other U-bearing minerals in some of the most important units of the rift.

The present paper describes a geochronological study in the Krokskogen area, in the northern Akershus Graben Segment of the Oslo Rift (Fig. 1). The study was aimed at resolving the timing of volcanic and plutonic events, but also testing some of the approaches to dating and evaluating the technical challenges connected to the dating of such rocks. The Krokskogen area is close to the the Krokkleiva-Kjaglidalen Transfer Fault, the tectonic accommodation zone between the Akershus Graben, which has an east-verging master fault on its western side, and the Vestfold Graben with the opposite subsidence polarity (Fig. 1; Larsen et al., 2008). Krokskogen exposes the complete and 900 m thick, classical plateau lava stratigraphy after Brøgger and

* Corresponding author.
E-mail address: corfu@geo.uio.no (F. Corfu).

https://doi.org/10.1016/j.lithos.2020.105755

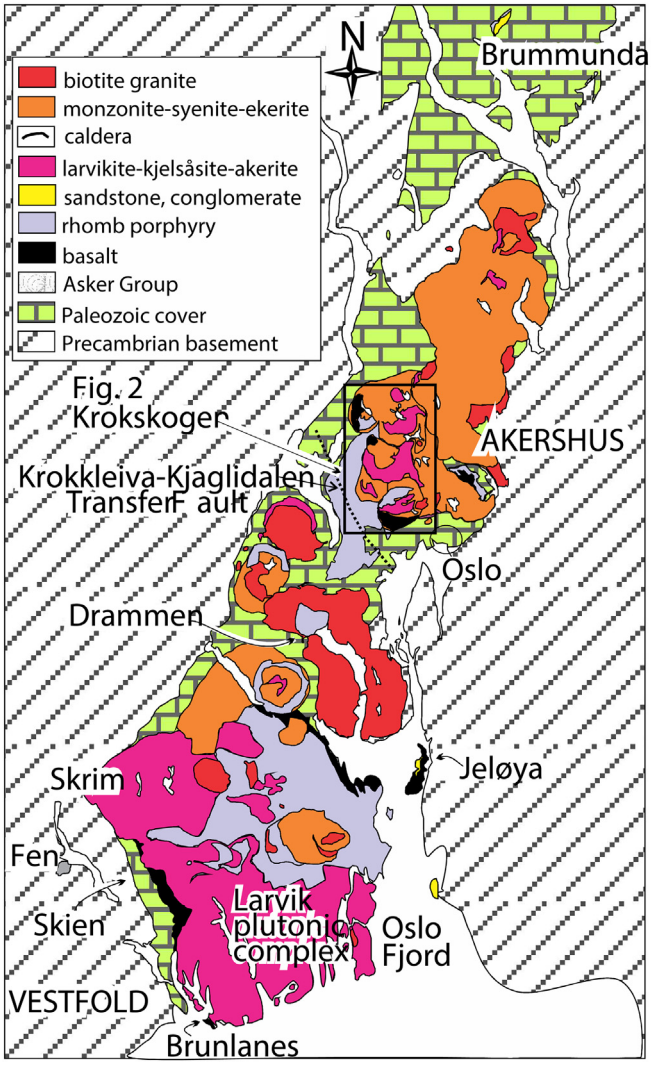

Fig. 1. Sketch map of the Oslo Graben with the two graben segments Vestfold and Akershus.

Schetelig (1917), Oftedahl (1952) and Larsen (1978). East of the plateau there is a north-trending string of calderas, again the most classical caldera volcanoes in the area (Oftedahl, 1953). In addition, there are various plutons, both older and younger than the calderas. The previous dating, mainly with Rb-Sr, had established the broad chronological framework, thus opening the opportunity to refine the time resolution using the U-Pb system.

2. Geological setting of Oslo Graben

The evolution of the Oslo Graben has been subdivided into six stages: (1) a proto-rift stage, (2) an initial basalt stage, (3) a main plateau-lava and rift-valley stage, (4) a central volcano and cauldron stage, (5) a syenitic batholiths stage, and (6) a termination stage (Larsen et al., 2008; Olaussen et al., 1994; Sundvoll and Larsen, 1994).

The proto-rift stage was characterized by deposition of the Asker Group, mainly fluvial and lacustrine sediments (Olaussen et al., 1994) and the local intrusion of syenitic sills (maenaite and some basic camptonites) (Corfu and Dahlgren, 2008a; Sundvoll et al., 1992; Sundvoll and Larsen, 1994).

This was followed by the initial-rift stage with mafic magmatism. Relatively thin (>5 m) basaltic flows in the southernmost parts comprise silica undersaturated melilitites and nephelinites dated by U-Pb at 300 Ma at Brunlanes and 299 Ma at Skien (Fig. 1; Corfu and Dahlgren, 2008b). Subsequent mafic volcanism (B1) erupted alkaline olivine basalt, up to 1500 m thick, in central parts of the graben, but only some 15 m of tholeiites at the Oslo latitude and none farther north (Neumann et al., 2004; Olaussen et al., 1994).

Stage 3 overlapped in time the late phases of basaltic magmatism and represented the initiation of rhomb porphyry eruptions from fissure volcanoes, especially in two areas, at Vestfold and Krokskogen, the latter the focus of the present paper (Figs. 1-2). The trachyandesitic rhomb porphyry lavas were likely related to the intrusion of large larvikite (monzonite) and nepheline syenite complexes, the Larvik plutonic complex dated at 299 to 292 Ma (Dahlgren et al., 1996) and the Skrim plutonic complex with ages of 281 to 277.3 Ma (Pedersen et al., 1995). Smaller larvikite-kjelsåsite (monzodioritic) intrusions are also present in the Krokskogen area and two have been dated in the present study.

Stage 4 involved the formation of central volcanoes and caldera collapse. The lavas ranged from alkaline olivine basalts to more Si-saturated transitional types (Larsen et al., 2008). The more fractionated ones consist of felsic, mostly trachytes to latites but also alkaline rhyolites with pyroclastic eruptions during the caldera formation. The volcanic complexes include ring dykes and central domes together with ignimbrites.

The fifth stage was characterized mainly by the emplacement of syenitic to granitic batholiths, especially in central and northern parts of the Oslo Rift, but both mafic magmas and rhomb porphyry magmas formed until late in this evolution and in part postdate the youngest felsic plutons (e.g. Nilsen, 1992).

3. Krokskogen

3.1. Rhomb porphyry sequence

The Krokskogen lava plateau covers about 400 km^2 and consists of a 900 m thick pile of flows erupted from long N-S-striking fissures. Rhomb porphyry lavas are the dominant elements. The flows vary in thickness and partly in distribution. Their eruption was interspersed with sporadic stages of basaltic magmatism and there were several periods of erosion with the deposition of interflow conglomerates and sandstones. The classical Krokskogen lava stratigraphy of Brøgger and Schetelig (1917) included twelve flows or flow units (RP1 to RP12). Subsequent mapping (Larsen, 1978; Larsen et al., 2008; Oftedahl, 1952; Ramberg and Larsen, 1978) added further subdivisions and refinements, so that presently the stratigraphic column consists of about 22 flow units, which are from 5 m to over 150 m thick and can include multiple individual flows. There are also RP lavas outside the lava plateau, inside the different calderas to the east. The whole stratigraphy starts with a tholeiitic basalt flow named B1, one of the three flows (B1 to B3) in the original classification. Subsequent mapping discovered another three flows, most of them in the upper part of the succession.

Rhomb porphyries are distinguished based on the density (5 to 30%), shape and size of the feldspar phenocrysts in a latitic to trachytic matrix. The phenocrysts are 0.5 to 3 cm in size and generally rhomb-shaped. They have a ternary composition and are zoned with Ca-rich core and K-rich rim (Harnik, 1969). The rhomb porphyries contain between 54 and 60% SiO_2 and relatively high contents of Na and K (9%), and carry subordinate clinopyroxene, magnetite and apatite in the matrix. The morphology of the flows indicates that the lavas must have been of low viscosity and flowed out from fissures over large areas. This has been attributed to high lava temperatures of about 1050–1100 °C (Larsen, 1978) and a high content of dissolved gases, especially F at 0.25 to 0.5% (Larsen et al., 2008).

3.2. Calderas

To the east of the lava plateau at Krokskogen there is a string of six calderas, partly nested into each other along an approximately

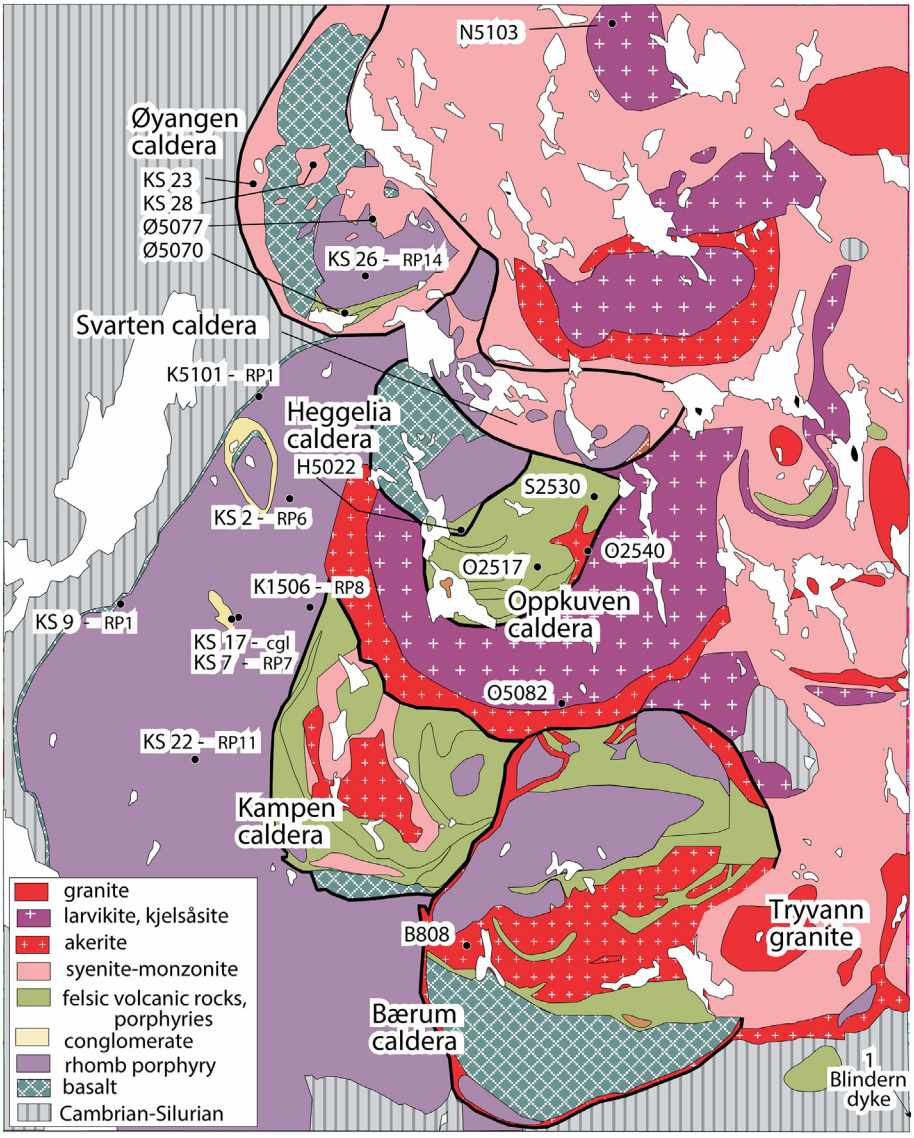

Fig. 2. Simplified geological map of the Krokskogen region showing main units and sample locations (based on Lutro and Nordgulen, 2004).

north-trending trajectory: the Bærum, Kampen, Oppkuven, Heggelia, Svarten and Øyangen calderas (Fig. 2; Oftedahl, 1953, 1978; Larsen, 1978). Geological evidence indicates that Øyangen is the youngest of the six. Several of the calderas have well developed, or remnants of, ring dykes, and also central dome intrusions. Inside the calderas are basaltic lavas, different types of felsic intrusions, and different types of felsic ignimbrites, both as clear extrusives, or as intrusion breccias. Some sediments also occur. Before collapsing, the calderas are inferred to have started as basaltic central volcanoes, of which only variable remnants are preserved. There are large volumes of basalt in the Øyangen, Heggelia, Kampen and Bærum calderas, but none in Oppkuven and just very little in Svarten. The ignimbrites vary in composition from trachytic in Øyangen, to more rhyolitic in Bærum and Oppkuven.

3.3. Other intrusions

Several smaller occurrences of larvikite and kjelsåsite are present in the region. Larvikite and kjelsåsite are distinguished on the basis of An content in plagioclase, An<30 and An>30, respectively, (Neumann, 1978).

Rhomb porphyry dykes are widespread in and around the main area of the Oslo Graben. Some are prominent dykes stretching for many tens of kilometers along major north-trending faults (Brøgger, 1933), whereas others are of more local significance. The latter author distinguishes earlier and younger rhomb porphyry dykes, the younger ones with more SiO_2 (58 vs 54%) but less Al_2O_3 (14 vs. 18%).

4. U-Pb geochronology

4.1. Samples

The initial aim of the study was to date the rhomb porphyry lavas and we collected samples representing the main stages of the sequence from RP1 to RP15. Several of the samples tested, however, did not contain any zircon or baddeleyite and the seven that could be analyzed had generally just few such minerals. Zircon was also recovered from a

mixture of clasts and sandy matrix of a conglomerate (Fjeldstadhytta) sandwiched between the RP6 and RP7 flows. The conglomerate was deposited by a coarse grained desert flash flow along a north-trending normal fault cutting the lava plateau. The coarse clasts were eroded from the RP lavas, and clasts of RP5, and subordinately of RP6, can be identified.

Nine other samples represent volcanic, subvolcanic and intrusive rocks from the Bærum, Oppkuven, Heggelia and Øyangen calderas. These samples have much better yields and quality of zircon than RPs, but for some exceptions. Another sample represents the 30 km^2 Slottet kjelsåsite pluton which surrounds the Oppkuven caldera. It is a coarse grained alkali monzonitic rock, with plagioclase of composition An35 and often coated with a thick alkali feldspar rim. Dark minerals are dominated by augite with subordinate biotite and apatite.

The two final samples represent late intrusives. The Tverrsjøen kjelsåsite (about 65 km^2; sample N5103; Fig. 2), located northeast of the Øyangen caldera, has been described by Sæther (1962) as a coarse grained "pulaskite", an alkali syenite consisting mainly of microperthitic to cryptoperthitic Na-rich feldspar, sodic pyroxene and amphibole, biotite and apatite. There is no plagioclase except in perthite, and no quartz. Petrographically it passes into nordmarkite (quartz-bearing alkali-feldspar syenite). Sample 1 (Fig. 2) is from a 2–3 m wide RP-like dyke cutting Ordovician limestone at Blindern, in the parking lot of the Geological Institute in Oslo. This dyke may correspond to the Natmandshougit dyke mentioned by Brøgger (1933), although at his type locality the latter exhibits fewer, smaller, and more fragmented feldspar phenocrysts.

4.2. Analytical procedure

Samples were crushed and pulverized before mineral concentration stages, which generally started with flotation on a Wilfley table, except for some of the rhomb porphyry samples that were processed by slow flotation in glass containers to avoid losing the very tiny grains of zircon and baddeleyite present, as observed in SEM images. Further enrichment of the heavy minerals was done with heavy liquids, magnetic separation, and finally hand picking. Selected zircons were generally subjected to chemical abrasion, adapted from Mattinson (2005), and involving a 3-days annealing stage at 900 °C followed by a ca. 17-h stage of partial dissolution in HF(+HNO_3) at about 180 °C. This partial dissolution turned out to be too extreme for some of the small, in part skeletal, and U-rich zircons. Other grains from these samples were then treated with air abrasion (Krogh, 1982), some subsequently followed by chemical abrasion with a shortened partial dissolution stage (Table 1). Baddeleyite was analyzed in three samples. Only a compact fragment of baddeleyite in one of the samples could be air abraded, the others were too small and flat crystals. In all three cases the results show clearly the effects of Pb loss.

Zircon and baddeleyite were dissolved in HF (+HNO_3) at 195 °C for about 5 days, thereafter converted to 3 N HCl and passed through anion exchange resin, except for the samples of less than 1 microgram. Titanite in one sample was dissolved on a hot plate, separating U and Pb with a 2-stage HBr-HCl-HNO_3 procedure. The samples were loaded on *Re*-filaments with H_3PO_4 and Si-gel and measured on a MAT 262 mass spectrometer, either in static multicollector mode or using an ion counting secondary electron multiplier. Further details of the procedure can be found in Corfu (2004). The data were corrected for ≤2 pg Pb and 0.1 pg U blanks. Any remaining common Pb was corrected using compositions calculated with the Stacey and Kramers (1975) model for the age of the sample. Fractionation of Pb was corrected using the $^{205}Pb/^{202}Pb$ ratio of the tracer and U with 0.12 ± 0.6%/amu, based on measurements of the U500 standard. Calculation was done using $^{238}U/^{235}U$ = 137.88 and the decay constants of Jaffey et al. (1971). Plotting and age calculations used the Isoplot program (Ludwig, 2009).

5. Results

5.1. Rhomb porphyry sequence

5.1.1. Rhomb porphyry RP1

Two samples were collected from RP1 flows. Sample KS 9 yielded just one zircon large enough to be analyzed. This was a thin prism, which after chemical abrasion gave a concordant analysis with an apparent age of 292.5 ± 1.0 Ma (Table 1, Fig. 3). The sample also contains baddeleyite, which, however, was too small to be analyzed. Four zircon fragments were recovered from the second sample (K5101); these had somewhat irregular but smooth exteriors, suggesting resorption. Three of the analyses are concordant with overlapping $^{206}Pb/^{238}U$ ages averaging 299.7 ± 0.4 Ma whereas the smallest fragment gives a distinctly younger date of about 279 Ma. The fact that the two younger analyses were obtained from small and thin crystals more susceptible to Pb loss, and the coherence of the three oldest analyses, support an interpretation of the 299.7 ± 0.4 Ma event as dating formation as RP1. The potential for an alternative consideration will be discussed below.

5.1.2. Rhomb porphyries RP6, RP7 and intervening conglomerate

The zircon extracted from sample KS2, representing RP6, consisted mainly of broken long prismatic crystals, mostly fractured and locally rusty. Chemical abrasion reduced them to small irregular fragments. A second batch of grains was air abraded, and one of them was given an additional short chemical abrasion treatment (Table 1). The analyses display a dispersion along the Concordia curve (Fig. 3). The oldest one, obtained from several scraps of zircon produced during chemical abrasion, could not be reproduced, and is unreliable. A younger group of four analyses defines an average $^{206}Pb/^{238}U$ age of 285.5 ± 0.8 Ma (MSWD = 1.9) and is considered the best estimate for the time of crystallization. Two other zircon data points are variously younger, likely due to their high U contents and imperfect crystal shapes, creating a relatively large surface with respect to the volume, which promoted partial Pb loss. Loss of Pb is also evident in the analysis of three small, unabraded grains of baddeleyite that gives a much younger age than the zircon crystals.

Sample KS7, representing RP7, yielded zircon qualitatively similar to those in KS2, i.e. broken and fractured prisms, partly rusty, especially along central channels parallel to the c-axis, and generally rich in U. Regular chemical abrasion almost fully destroyed the grains, and subsequent attempts were done with air abrasion, in part combined with a mild chemical abrasion treatment (Table 1). The resulting analyses show some spread, likely a consequence of some Pb loss. The $^{206}Pb/^{238}U$ ages of the five oldest data points have an average of 284.1 ± 1.0 Ma, but with a MSWD of 5.7. The two oldest analyses average 284.9 ± 0.5 Ma (MSWD = 0.08). An attempt was also made with baddeleyite, but the result is partially reset.

The zircon population extracted from the intervening conglomerate consists mainly of well rounded zircon grains, but a small amount of sharp euhedral crystals is also present. The latter are short prismatic to equant, have a dominant development of {100} and {101} faces, and generally contain inclusions of melt or dark minerals. Three of analyses give ages older than 295 Ma (Table 1). Seven other points have $^{206}Pb/^{238}U$ ages between 286.5 ± 0.8 Ma and 284.0 ± 1.1 Ma. Another grain yields a date of 282.8 Ma, which is younger than the age of the overlying flow and thus suspected to be affected by Pb loss. The data cluster is broadly consistent with the ages of the bracketing flows. The youngest age of this group would normally be regarded to most closely approach the time of deposition, but because of the evidence of some Pb loss in this population some residual uncertainty remains.

5.1.3. Rhomb porphyry RP11

Sample KS 22 (RP11) provided a zircon population of somewhat better quality than in the other rhomb porphyries investigated. The zircons

Table 1
U-Pb data.

Properties	Weight	U	Th/U[c]	Pbc	206/204[e]	207/235[f]	2 sigma	206/238[f]	2 sigma	rho	207/206[f]	2 sigma	206/238[f]	2 sigma	207/235[f]	2 sigma	207/206[f]	2 sigma
	[ug][a]	[ppm][b]		[pg][d]			[abs]		[abs]			[abs]		[abs]		[abs]		[abs]
K-5101 – RP1 – Krokskogen lava plateau, Nordre Gaupeskar, Ringerike, 60.10728 10.38505																		
Z an irreg CA [1]	1	209	0.80	0.6	1002	0.34293	0.00187	0.04749	0.00014	0.60	0.05237	0.00023	299.1	0.9	299.4	1.4	301.8	9.9
Z an smooth CA [1]	1	191	0.86	0.5	1038	0.34296	0.00167	0.04763	0.00012	0.60	0.05223	0.00020	299.9	0.8	299.4	1.3	295.3	8.9
Z an irreg CA [1]	15	87	0.75	1.0	3803	0.34283	0.00113	0.04760	0.00011	0.86	0.05224	0.00009	299.7	0.7	299.3	0.9	295.9	4.1
Z an fr CA [1]	1	119	0.67	1.6	215	0.31768	0.00608	0.04428	0.00016	0.30	0.05203	0.00096	279.3	1.0	280.1	4.7	286.7	41.5
KS 9 – RP1 – Krokskogen lava plateau, Dronningveien, Hole, 60.052972 / 10.321972 (KS-9-12)																		
Z lp fr CA [1]	1	188	2.24	1.2	483	0.33307	0.00526	0.04642	0.00017	0.46	0.05203	0.00075	292.5	1.0	291.9	4.0	286.9	32.8
KS 2 – RP6 – Krokskogen lava plateau, Bridge Lomma, Fjellseterbommen, Ringerike, 60.082667 / 10.401472 (KS-2-12)																		
Z lp fr CA [5]	1	80	0.94	1.1	231	0.32292	0.01102	0.04585	0.00021	0.49	0.05108	0.00164	289.0	1.3	284.1	8.4	244.3	72.4
Z lp fr CA [3]	1	232	1.45	0.9	781	0.32723	0.00324	0.04540	0.00012	0.50	0.05227	0.00046	286.2	0.7	287.4	2.5	297.3	20.1
Z lp fr AA [1]	1	348	1.92	0.2	4005	0.32407	0.00122	0.04525	0.00010	0.67	0.05194	0.00015	285.3	0.6	285.0	0.9	282.7	6.4
Z lp fr AA [1]	1	668	2.41	0.6	2985	0.32444	0.00120	0.04524	0.00012	0.76	0.05201	0.00013	285.2	0.7	285.3	0.9	285.9	5.5
Z lp fr CA [1]	1	143	1.30	2.5	183	0.32378	0.01159	0.04522	0.00018	0.54	0.05194	0.00175	285.1	1.1	284.8	8.9	282.6	75.5
Z lp fr AA [1]	1	522	2.25	0.3	4803	0.32280	0.00103	0.04510	0.00010	0.79	0.05191	0.00010	284.4	0.6	284.1	0.8	281.2	4.5
Z lp fr AA-CA* [1]	1	722	2.63	7.2	294	0.31324	0.00233	0.04419	0.00012	0.50	0.05141	0.00033	278.8	0.7	276.7	1.8	259.1	14.9
B lp NA [3]	1	236	0.24	2.0	319	0.29918	0.00682	0.04117	0.00011	0.55	0.05270	0.00113	260.1	0.7	265.8	5.3	315.9	48.0
KS 17 – Conglomerate between RP6 and RP7, Krokskogen lava plateau, (Fjeldstadhytta), Fjellseterveien, Bjørkevad junction, Ringerike, 60.055306 / 10.381778)KS-17–12)																		
Z sp. fr CA [1]	2	364	0.37	0.6	12,641	1.74365	0.00785	0.16502	0.00056	0.83	0.07663	0.00020	984.6	3.1	1024.8	2.9	1111.7	5.1
Z tip fr CA [1]	6	61	0.55	0.7	2693	0.70121	0.00321	0.07734	0.00020	0.67	0.06576	0.00023	480.2	1.2	539.5	1.9	798.7	7.2
Z sp. fr CA [1]	2	62	1.12	0.9	424	0.35446	0.00313	0.04686	0.00011	0.48	0.05486	0.00044	295.2	0.7	308.1	2.3	406.7	17.7
Z eq. CA [1]	5	28	0.72	0.4	981	0.32357	0.00269	0.04544	0.00013	0.48	0.05165	0.00038	286.5	0.8	284.6	2.1	269.8	16.9
Z sp. fr CA [1]	8	215	0.99	1.0	4993	0.32632	0.00117	0.04544	0.00012	0.82	0.05209	0.00011	286.4	0.7	286.8	0.9	289.3	4.8
Z eq. CA [1]	9	39	0.86	11.4	106	0.33100	0.01157	0.04541	0.00021	0.24	0.05286	0.00181	286.3	1.3	290.3	8.8	323.0	75.8
Z sp. fr CA [1]	4	83	1.03	1.0	1002	0.32473	0.00190	0.04538	0.00010	0.61	0.05190	0.00025	286.1	0.6	285.5	1.5	281.0	10.9
Z eq. CA [1]	2	103	0.80	0.9	659	0.32234	0.00341	0.04528	0.00011	0.48	0.05162	0.00050	285.5	0.6	283.7	2.6	268.8	22.1
Z eq. CA [1]	8	39	1.01	3.3	287	0.32569	0.00591	0.04516	0.00015	0.47	0.05230	0.00088	284.8	0.9	286.3	4.5	298.6	38.0
Z eq. CA [1]	1	950	0.87	1.2	2287	0.32358	0.00189	0.04504	0.00017	0.74	0.05211	0.00021	284.0	1.1	284.7	1.4	290.2	9.0
Z tip fr CA [1]	2	327	0.81	0.5	3579	0.32150	0.00130	0.04485	0.00013	0.79	0.05199	0.00013	282.8	0.8	283.1	1.0	285.1	5.7
KS 7 – RP7 – Krokskogen lava plateau, Fjellseterveien, Bjørkevad junction, Ringerike, Ringerike, 60.054528 / 10.382417 (KS-7-12)																		
Z lp fr AA [1]	1	821	1.83	1.6	1509	0.32285	0.00111	0.04520	0.00011	0.80	0.05180	0.00011	285.0	0.7	284.1	0.9	276.7	4.8
Z lp fr AA [1]	1	624	1.89	0.2	7722	0.32259	0.00106	0.04518	0.00010	0.75	0.05178	0.00011	284.9	0.6	283.9	0.8	275.9	5.0
Z lp fr AA-CA* [1]	1	637	1.55	1.0	1758	0.32164	0.00134	0.04501	0.00011	0.75	0.05183	0.00015	283.8	0.7	283.2	1.0	277.7	6.5
Z lp fr CA [1]	1	129	1.55	0.9	423	0.32027	0.00607	0.04494	0.00014	0.48	0.05169	0.00091	283.4	0.8	282.1	4.7	271.7	40.1
Z lp fr AA [1]	1	602	1.88	0.2	7351	0.32193	0.00121	0.04492	0.00011	0.71	0.05198	0.00014	283.3	0.7	283.4	0.9	284.3	6.1
Z lp fr CA [10]	1	1482	1.43	1.6	2695	0.32173	0.00123	0.04486	0.00010	0.67	0.05201	0.00015	282.9	0.6	283.2	0.9	285.9	6.5
Z lp fr AA-CA* [1]	1	371	1.72	0.8	1293	0.31900	0.00128	0.04449	0.00011	0.80	0.05200	0.00013	280.6	0.7	281.1	1.0	285.5	5.8
Z lp fr AA-CA* [1]	1	59	1.36	0.8	184	0.27022	0.00653	0.03808	0.00013	0.54	0.05147	0.00116	240.9	0.8	242.9	5.2	261.9	50.8
B lp NA [2]	1	331	0.11	0.8	1100	0.31611	0.00248	0.04391	0.00015	0.57	0.05221	0.00034	277.1	0.9	278.9	1.9	294.5	14.9
K1506 – RP8 – Krokskogen lava plateau, North Monsebråtan, Ringerike, 60.05859 / 10.41309																		
Z an fr CA [1]	1	43	0.00	0.5	554	0.81824	0.00661	0.09731	0.00035	0.52	0.06098	0.00042	598.6	2.1	607.1	3.7	638.6	14.8
Z an fr CA [1]	1	617	1.30	0.5	3540	0.30004	0.00108	0.04215	0.00011	0.77	0.05163	0.00012	266.2	0.7	266.4	0.8	268.9	5.3
KS 22 – RP11 – Krokskogen lava plateau, Kongeveien quarry, Hole, 60.0191675 / 10.3638929 (KS-22–12)																		
Z eu fr AA [1]	1	493	1.34	1.1	1301	0.31790	0.00216	0.04453	0.00013	0.58	0.05177	0.00029	280.9	0.8	280.3	1.7	275.4	12.9
Z eu fr AA [3]	1	1702	1.42	1.4	3408	0.31766	0.00129	0.04440	0.00011	0.77	0.05189	0.00014	280.1	0.7	280.1	1.0	280.4	6.1
Z eu fr AA [1]	1	1766	1.44	4.8	1035	0.31763	0.00164	0.04429	0.00014	0.67	0.05201	0.00020	279.4	0.8	280.1	1.3	285.8	8.7
Z eu lp fr CA [1]	1	408	0.97	0.7	1527	0.30971	0.00202	0.04330	0.00016	0.67	0.05188	0.00026	273.2	1.0	274.0	1.6	280.0	11.2
KS 26 – RP14 – Øyangen caldera, Hægåsveien, Ringkollen, Ringerike, 60.136500 / 10.425278 (KS-26-12)																		
B tip AA [1]	1	110	0.33	2.6	125	0.28550	0.01453	0.03978	0.00019	0.59	0.05205	0.00251	251.5	1.2	255.0	11.4	287.5	106.8

(continued on next page)

Table 1 (*continued*)

Properties	Weight [ug][a]	U [ppm][b]	Th/U[c]	Pbc [pg][d]	206/204[e]	207/235[f]	2 sigma [abs]	206/238[f]	2 sigma [abs]	rho	207/206[f]	2 sigma [abs]	206/238[f]	2 sigma [abs]	207/235[f]	2 sigma [abs]	207/206[f]	2 sigma [abs]
B808 – Akerite (monzonite), central pluton, Bærum caldera, Burudvann, Haugen, Bærumsmarka, 59.97564 / 10.50775																		
Z fr CA [1]	1	1087	0.73	0.5	6403	0.31505	0.00129	0.04402	0.00015	0.92	0.05191	0.00008	277.7	0.9	278.1	1.0	281.3	3.7
Z fr CA [1]	1	326	1.94	0.3	3241	0.31382	0.00118	0.04381	0.00011	0.83	0.05195	0.00011	276.4	0.7	277.1	0.9	283.2	4.9
Z an eq. CA [1]	1	175	1.02	0.7	651	0.31371	0.00229	0.04378	0.00017	0.61	0.05197	0.00030	276.2	1.0	277.1	1.8	284.1	13.2
H5022 – Trachyte ignimbrite, red, Heggelia caldera, Heggeliveien, Nordre Heggelivann, Ringerike, 60.07664 10.48347																		
Z eu sp. CA [3]	6	136	0.84	1.1	1987	0.31450	0.00128	0.04391	0.00010	0.73	0.05194	0.00015	277.0	0.6	277.7	1.0	283.0	6.5
Z tips CA [5]	13	108	0.86	2.5	1508	0.31417	0.00139	0.04382	0.00011	0.73	0.05200	0.00016	276.5	0.7	277.4	1.1	285.2	7.1
Z eu sp. CA [2]	4	140	0.84	1.0	1560	0.31377	0.00154	0.04377	0.00011	0.67	0.05199	0.00019	276.2	0.7	277.1	1.2	284.9	8.5
O2540 – Syenite, Stuevann type (ring dyke), Oppkuven caldera, Ringerike, Stuevann, SE Oppkuven, Ringerike, 60.07522 / 10.55227																		
Z fr AA pk [1]	8	2212	0.88	1.0	49,022	0.32149	0.00084	0.04503	0.00010	0.96	0.05178	0.00004	283.9	0.6	283.0	0.6	275.7	1.7
Z lp fr CA [3]	13	433	0.76	1.7	8934	0.31295	0.00088	0.04384	0.00010	0.88	0.05177	0.00007	276.6	0.6	276.5	0.7	275.3	3.1
Z lp fr CA [1]	7	748	0.85	0.6	23,223	0.31323	0.00079	0.04377	0.00009	0.91	0.05190	0.00005	276.2	0.6	276.7	0.6	280.9	2.4
Z lp fr CA [4]	9	700	0.64	1.1	14,894	0.31235	0.00088	0.04370	0.00010	0.90	0.05184	0.00006	275.7	0.6	276.0	0.7	278.4	2.8
Z fr AA rd [1]	4	8743	0.42	1.5	62,464	0.31231	0.00075	0.04370	0.00009	0.97	0.05183	0.00003	275.7	0.6	276.0	0.6	278.1	1.5
Z lp fr CA [7]	13	695	0.84	8.7	2798	0.31039	0.00090	0.04362	0.00010	0.85	0.05161	0.00008	275.2	0.6	274.5	0.7	268.0	3.5
Z lp fr CA [6]	18	589	0.85	0.8	33,909	0.31101	0.00080	0.04355	0.00009	0.92	0.05179	0.00005	274.8	0.6	275.0	0.6	276.2	2.3
Z fr AA pk [1]	1	4562	0.91	1.4	8938	0.31120	0.00088	0.04354	0.00010	0.90	0.05184	0.00007	274.7	0.6	275.1	0.7	278.2	2.9
S2530 - Grey porphyry / trachyte lava, Oppkuven caldera, Heggeliveien, nordre Gopletjern, Stuevann, Ringerike, 60.08776 / 10.55118																		
Z eu eq. CA [1]	12	192	0.54	1.6	3843	0.31534	0.00114	0.04426	0.00011	0.79	0.05167	0.00011	279.2	0.7	278.3	0.9	270.8	5.1
Z eu sp. CA [1]	12	76	0.53	1.0	2550	0.31485	0.00127	0.04419	0.00012	0.79	0.05168	0.00013	278.7	0.7	277.9	1.0	271.1	5.8
Z fr CA [4]	8	110	0.47	6.3	397	0.31457	0.00326	0.04418	0.00012	0.38	0.05164	0.00050	278.7	0.7	277.7	2.5	269.4	22.0
Z eu tips CA [6]	12	187	0.57	2.3	2686	0.31390	0.00107	0.04404	0.00010	0.77	0.05169	0.00011	277.8	0.6	277.2	0.8	271.9	5.0
Z eu tip CA [1]	13	84	0.49	5.6	550	0.31464	0.00267	0.04384	0.00011	0.46	0.05205	0.00040	276.6	0.7	277.8	2.1	287.6	17.4
Z eu tips CA [2]	12	114	0.56	1.8	2098	0.31209	0.00146	0.04366	0.00010	0.66	0.05185	0.00019	275.5	0.6	275.8	1.1	278.6	8.3
T fr br NA [6]	73	152	3.23	84.8	371	0.31384	0.00298	0.04388	0.00011	0.34	0.05187	0.00046	276.8	0.7	277.2	2.3	279.9	20.3
T fr br NA [12]	78	132	3.17	72.8	399	0.31046	0.00268	0.04373	0.00010	0.33	0.05149	0.00042	275.9	0.6	274.5	2.1	262.8	18.6
O2517 – Rhyolitic ignimbrite, Oppkuven Caldera, Kjagdalen, nordre Gopletjern, Ringerike, 60.06727 / 10.52656																		
Z eu sp. CA [3]	12	80	0.53	4.0	682	0.31969	0.00204	0.04458	0.00013	0.57	0.05201	0.00028	281.2	0.8	281.7	1.6	285.9	12.0
Z fr CA [1]	2	260	0.46	5.2	289	0.31653	0.00595	0.04433	0.00014	0.37	0.05179	0.00093	279.6	0.9	279.2	4.6	276.1	40.4
Z fr CA [4]	59	202	0.84	2.4	13,191	0.31333	0.00078	0.04382	0.00009	0.94	0.05186	0.00005	276.5	0.6	276.8	0.6	279.4	2.0
Z fr CA [4]	23	332	0.97	1.1	19,298	0.31328	0.00083	0.04379	0.00009	0.90	0.05189	0.00006	276.3	0.6	276.7	0.6	280.7	2.7
Z fr CA [8]	35	128	0.76	1.8	6773	0.30985	0.00095	0.04337	0.00009	0.77	0.05181	0.00010	273.7	0.6	274.1	0.7	277.2	4.5
KS 23 – Syenite, Ring Dyke, Øyangen caldera, Ringkollveien bommen, Ringerike, 60.158472 / 10.370472 (KS-23-12)																		
Z eu eq. CA [4]	2	417	0.35	1.4	1605	0.30938	0.00113	0.04343	0.00010	0.74	0.05166	0.00013	274.1	0.6	273.7	0.9	270.4	5.7
Z eu eq. CA [5]	2	502	0.32	1.4	2023	0.30959	0.00109	0.04340	0.00010	0.77	0.05173	0.00012	273.9	0.6	273.9	0.8	273.6	5.2
Z eu eq. CA [1]	1	127	0.43	0.9	388	0.30873	0.00262	0.04325	0.00012	0.56	0.05177	0.00038	272.9	0.8	273.2	2.0	275.3	16.5
Z eu eq-sp CA [15]	20	154	0.38	1.2	6772	0.30845	0.00081	0.04322	0.00008	0.84	0.05176	0.00007	272.8	0.5	273.0	0.6	274.8	3.3
Z eu eq. CA [12]	14	94	0.45	2.9	1259	0.30752	0.00170	0.04317	0.00010	0.62	0.05166	0.00023	272.5	0.6	272.3	1.3	270.4	10.2
Z eu eq. CA [1]	1	225	0.36	0.8	791	0.30767	0.00211	0.04313	0.00018	0.67	0.05174	0.00026	272.2	1.1	272.4	1.6	273.8	11.6
Z eu sq. CA [1]	1	587	0.31	1.1	1514	0.30691	0.00109	0.04310	0.00011	0.81	0.05165	0.00011	272.0	0.7	271.8	0.8	269.7	4.8
Z eu eq. CA [18]	20	231	0.35	3.1	4087	0.30797	0.00086	0.04307	0.00009	0.82	0.05186	0.00008	271.8	0.5	272.6	0.7	279.2	3.7
Z eu eq. CA [14]	14	206	0.36	2.4	3324	0.30827	0.00102	0.04305	0.00009	0.73	0.05194	0.00012	271.7	0.6	272.8	0.8	282.7	5.2
KS 28 – Syenite, Central Complex, Øyangen caldera, Ringkolltoppen, Ringerike, 60.166389 / 10.400556 (KS-28-12)																		
Z lp-fr CA [1]	1	124	0.73	1.1	325	0.31259	0.00731	0.04332	0.00019	0.45	0.05234	0.00114	273.4	1.2	276.2	5.6	300.1	48.8
Z an eq. CA [6]	6	112	0.73	1.3	1441	0.30848	0.00193	0.04319	0.00009	0.48	0.05180	0.00029	272.6	0.5	273.0	1.5	276.6	12.7
Z lp-fr CA [1]	1	100	0.71	3.8	89	0.31285	0.01812	0.04315	0.00025	0.50	0.05258	0.00291	272.3	1.5	276.4	13.9	310.8	121.1
Z an sp. CA [1]	1	643	0.72	0.5	3184	0.29341	0.00121	0.04137	0.00009	0.73	0.05144	0.00015	261.3	0.6	261.2	0.9	260.6	6.6
Z an sp. CA [1]	1	321	0.67	2.0	412	0.28228	0.00506	0.03971	0.00014	0.45	0.05155	0.00086	251.0	0.9	252.5	4.0	265.7	37.6

eru- ing dur- dy rea- al- or rock the of ng shi- cru- ing dur- ed tur- frac- they er eth- wh- tain cer- un- it is but s, stal- cry- al gin- ori- the of on uti- stit- con- cate deli- the to rily ma- pri- d late- re- is ring tu- frac- The ms. pris- dral he- eu- ken bro- stly mo- re we-

Ø5077 – Rhyolitic ignimbrite, Øyangen caldera, East Rughaug, Ringerike, 60.1528 / 10.42919 (Ø-5077B)																		
Z eu tips+fr CA [5]	20	200	0.54	1.2	9158	0.31114	0.00118	0.04374	0.00012	0.83	0.05159	0.00011	276.0	0.8	275.1	0.9	267.4	4.9
Z eu tips CA [2]	16	266	0.70	1.2	9671	0.31204	0.00079	0.04367	0.00009	0.88	0.05182	0.00006	275.5	0.5	275.8	0.6	277.7	2.8
Z eu sp. CA [1]	14	423	1.00	0.7	24,015	0.31098	0.00080	0.04353	0.00010	0.93	0.05181	0.00005	274.7	0.6	274.9	0.6	276.9	2.1
Z eu lp-fr CA [4]	25	263	0.48	1.3	13,826	0.30985	0.00079	0.04340	0.00009	0.88	0.05178	0.00006	273.9	0.5	274.1	0.6	275.6	2.8
Z eu eq. CA [5]	34	344	0.79	1.0	29,989	0.30801	0.00077	0.04324	0.00010	0.95	0.05166	0.00004	272.9	0.6	272.6	0.6	270.3	1.8
Ø5070 – Rhyolite tuff, Øyangen caldera, Damtjern north shore, Ringerike, 60.12833 / 10.41926 (Ø-5070A)																		
Z sb eq. CA [1]	1	458	0.66	0.6	18,562	10.00140	0.04104	0.39967	0.00154	0.98	0.18149	0.00017	2167.5	7.1	2434.9	3.8	2666.5	1.5
Z eu sp. CA [1]	1	380	0.40	1.3	4059	2.61735	0.00835	0.22049	0.00059	0.90	0.08609	0.00012	1284.5	3.1	1305.5	2.3	1340.3	2.7
Z eu sp. CA [1]	1	301	0.29	2.2	661	0.65474	0.00401	0.07684	0.00027	0.67	0.06180	0.00028	477.2	1.6	511.4	2.5	667.3	9.7
O5082 – Kjelsåsite, Slottet pluton, Stuteskallen, vest Lysedammene, Sørkedalen, 60.03533 / 10.54726																		
Z eu eq. CA [6]	30	128	0.66	4.0	2633	0.31683	0.00092	0.04428	0.00009	0.78	0.05189	0.00009	279.3	0.6	279.5	0.7	280.6	4.2
Z eu tips CA [2]	12	148	0.72	6.7	730	0.31091	0.00176	0.04389	0.00009	0.47	0.05138	0.00026	276.9	0.6	274.9	1.4	257.9	11.5
Z eu tips CA [3]	21	175	0.68	6.4	1556	0.31326	0.00110	0.04387	0.00010	0.74	0.05179	0.00012	276.8	0.6	276.7	0.9	276.0	5.5
Z eu sp. CA [3]	13	118	0.77	2.7	1540	0.31383	0.00118	0.04382	0.00009	0.64	0.05194	0.00015	276.5	0.6	277.1	0.9	282.6	6.6
Z eu sp. CA [6]	39	216	0.62	16.8	1370	0.31143	0.00133	0.04382	0.00011	0.68	0.05154	0.00016	276.5	0.7	275.3	1.0	265.2	7.2
Z eu eq. CA [2]	29	133	0.63	5.2	2009	0.31341	0.00113	0.04377	0.00010	0.73	0.05193	0.00013	276.2	0.6	276.8	0.9	282.4	5.7
N5103 – Kjelsåsite (monzodiorite) pluton, rock quarry, East Tverrsjøen, Jevnaker, 60.20754 / 10.5392																		
Z fr CA [4]	35	236	1.60	3.2	6654	0.29914	0.00078	0.04211	0.00009	0.89	0.05152	0.00006	265.9	0.5	265.7	0.6	264.3	2.7
Z lp-fr CA [1]	10	301	1.34	0.3	23,387	0.29857	0.00069	0.04207	0.00008	0.93	0.05148	0.00005	265.6	0.5	265.3	0.5	262.3	2.0
Z lp-fr CA [1]	10	203	1.38	1.0	5473	0.29768	0.00086	0.04199	0.00008	0.78	0.05141	0.00009	265.2	0.5	264.6	0.7	259.5	4.2
Z fr CA [5]	45	150	1.26	3.6	4873	0.29807	0.00080	0.04197	0.00009	0.86	0.05151	0.00007	265.0	0.5	264.9	0.6	263.9	3.2
1 – Rhomb porphyry-like dyke, Blindern (C-14-1)																		
Z eu tips CA [11]	69	31	1.67	2.0	2815	0.29555	0.00139	0.04163	0.00009	0.54	0.05149	0.00020	262.9	0.5	262.9	1.1	263.0	9.1
Z eu sp. CA [5]	48	35	1.74	1.6	2703	0.29496	0.00142	0.04149	0.00010	0.65	0.05156	0.00019	262.1	0.6	262.5	1.1	265.9	8.5
Z eu sp-fr CA [10]	48	35	1.46	1.4	3110	0.29525	0.00089	0.04153	0.00009	0.81	0.05156	0.00009	262.3	0.6	262.7	0.7	266.0	4.1
Z eu sp. CA [4]	65	18	1.56	2.0	1492	0.29446	0.00096	0.04153	0.00009	0.75	0.05143	0.00011	262.3	0.5	262.1	0.8	260.1	5.0
Z eu fr CA [17]	197	28	1.68	4.8	3006	0.29403	0.00083	0.04145	0.00008	0.81	0.05145	0.00009	261.8	0.5	261.7	0.7	260.9	3.9

[a] Z = zircon; B = baddeleyite; T = titanite; eu = euhedral; sb = subhedral; an = anhedral; lp = long prismatic; eq = equant; sp. = short prismatic; fr = fragment; irreg = irregular; br = brown; [N] = number of grains in fraction; CA = chemically abraded; CA* = partial dissolution time reduced to 3 h from normally about 17 h; AA = air abraded

[b] Weight and concentrations are known to better than 10%, except for those near and below the ca. 1 μg limit of resolution of the balance.

[c] Th/U model ratio inferred from 208/206 ratio and age of sample

[d] Pbc = total common Pb in sample (initial +blank)

[e] Raw data corrected for fractionation and spike

[f] Corrected for fractionation, spike, blank (206/204 = 18.07 (0.56%), 207/204 = 15.57 (0.4%)) and initial common Pb (based on Stacey and Kramers, 1975); error calculated by propagating the main sources of uncertainty.

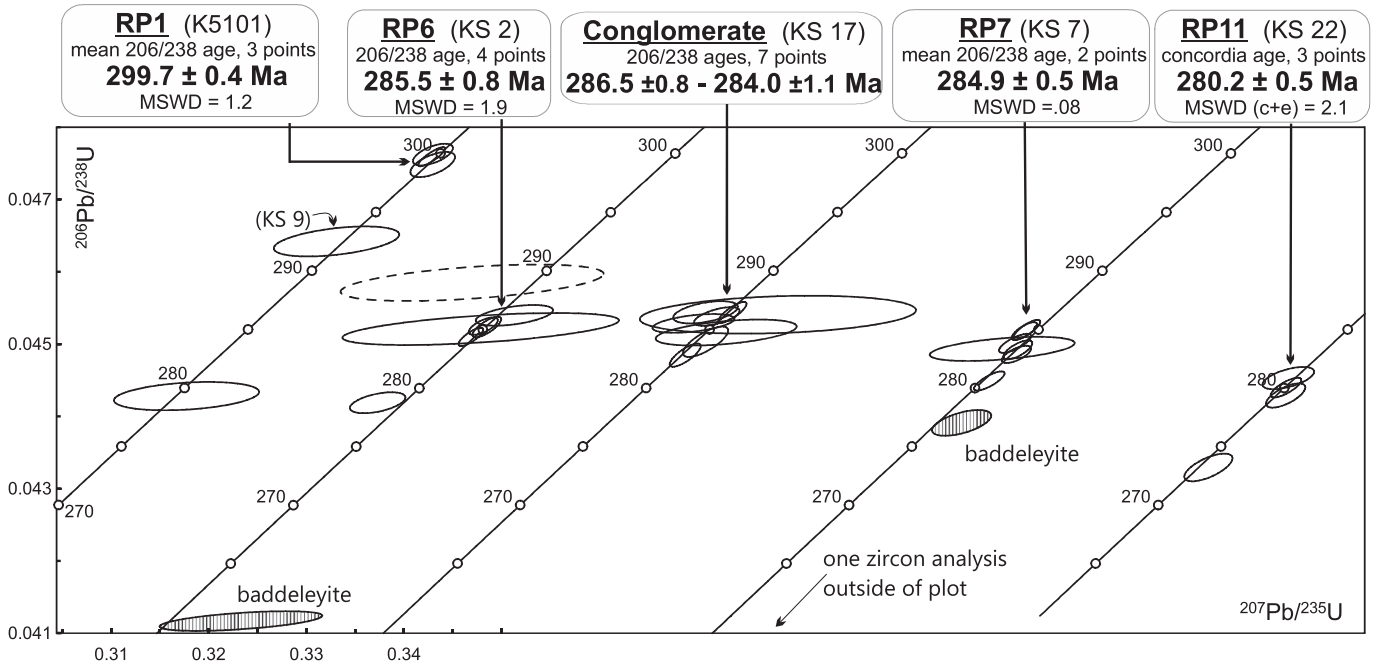

Fig. 3. Concordia plots with U-Pb data of the rhomb porphyry sequence.

ption. The results also exhibit the effects of some Pb loss, specifically the analysis of a chemically abraded grain, likely due to local fracturing. Three other grains treated by air abrasion yield overlapping concordant data giving a concordia age of 280.2 ± 0.5 Ma. Baddeleyite is also present, but in the form of small platy grains, and was not analyzed.

5.1.4. Unsuccessful attempts with other rhomb porphyry samples

Sample K1506, representing RP8, yielded just few zircon fragments, of which two could be analyzed (Table 1). One is discordant, indicating an age older than 600 Ma, hence of exotic provenance. The second analysis yields an apparent age of 266 Ma, concordant but likely partially reset by Pb loss.

From sample KS 26, representing RP14, several baddeleyite blades and few zircon grains were recovered, but these grains did not fare well through the next analytical steps. The zircon grains did not survive the chemical abrasion step. Baddeleyite was air abraded to remove the external domains affected by Pb loss. That process, however, destroyed most of the grains. Only one grain was analyzed and it provides an apparent age of 251 Ma, which is considered to be partially reset. In several other cases no zircon or baddeleyite could be recovered. This includes additional samples of RP6, RP8, RP11 (2×), basalt B2, RP10 (2×) and RP15.

5.2. Calderas and coeval plutons

5.2.1. Bærum caldera

The Bærum caldera is represented by a sample of akerite (quartz monzonite) B808 from the central complex. Only three small zircon grains were recovered from this sample. Their analyses gave essentially concordant and overlapping data with an average $^{206}Pb/^{238}U$ age of 276.7 ± 1.8 Ma (Table 1, Fig. 4).

5.2.2. Heggelia caldera

The syenite to trachyte sample H5022 from the central pluton had a good zircon population of sharp euhedral crystals, ranging from equant to long prismatic, with a pronounced development of the {100} and {101} crystal faces and many inclusions of other minerals. Three analyses of short prismatic grains and of fragments yield overlapping data defining a $^{206}Pb/^{238}U$ age of 276.6 ± 1.1 Ma.

5.2.3. Oppkuven caldera

Zircons in syenite sample O2540 were predominantly broken prisms, highly fractured, with many inclusions of other minerals such as biotite (as observed under the microscope), mostly oriented along the c-axis. There is also a subpopulation of brown to pink zircons, very rich in U. One of these grains gives an apparent age of about 283 Ma, distinctly older than the main cluster, and of uncertain significance. The other seven analyses of chemically and air abraded zircons show some scatter in apparent ages between 277 and 274 Ma, whereby the more fractured grains yielded slightly lower dates pointing to some Pb loss. Five analyses provide an average $^{206}Pb/^{238}U$ age of 275.9 ± 0.6 Ma (MSWD = 3.0).

Sample S2530 is a grey porphyry to trachyte lava containing an assortment of zircon types, mostly euhedral and short prismatic but also fragments, and with common inclusions of other minerals. Six zircon analyses are spread over a range of 4 m.y. whereby the two youngest ones, obtained from zircon tips, overlap with two analyses of titanite. The average $^{206}Pb/^{238}U$ age of this group, 276.1 ± 1.0 Ma, is interpreted as the emplacement age of the subvolcanic unit, while the older analyses likely reflect the presence either of antecrysts or of inherited cores.

The third sample from the Oppkuven caldera, a rhyolitic ignimbrite O2517, provided a zircon population dominated by fragments with a minor amount of euhedral short-prismatic crystals. The five analyses show a wide scatter in ages with two at about 280 Ma, two at 276.4 Ma and one at about 274 Ma. In this case the selected zircon characteristics offer no simple rationale for explaining the data pattern. The analogy with the two other samples in this caldera suite suggests, however, that 276.4 Ma could represent the magmatic generation with the older group representing xenocrysts while the younger would have to be explained in terms of Pb loss.

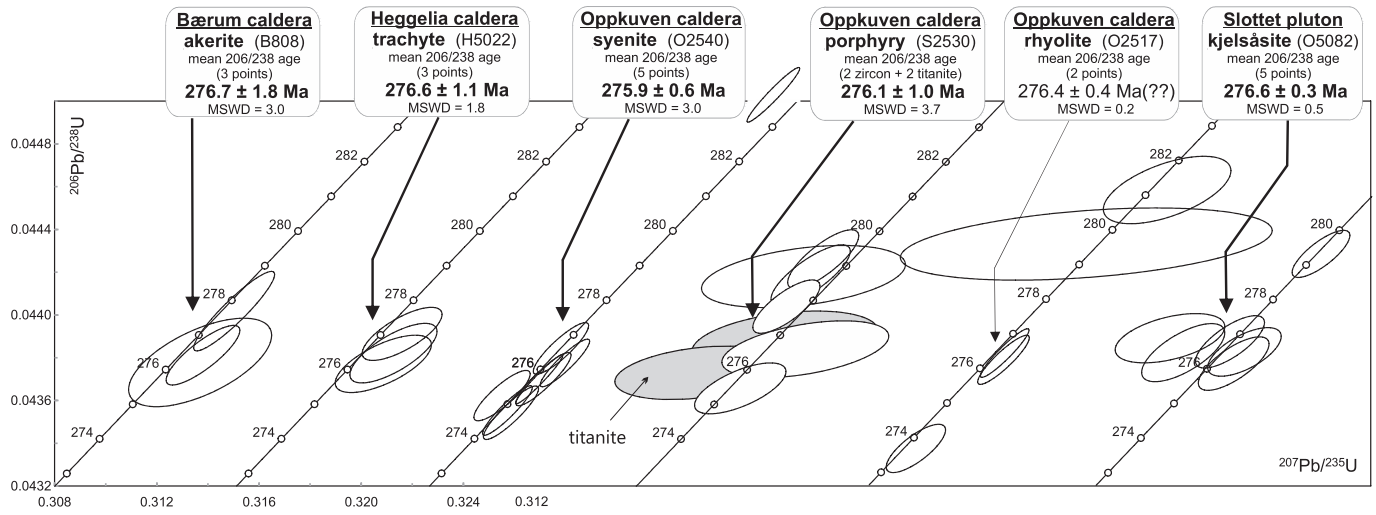

Fig. 4. Concordia plots with U-Pb data of the Bærum, Oppkuven and Heggelia calderas and the Slottet kjelsåsite.

5.2.4. Slottet kjelsåsite

Sample O5082 of kjelsåsite, from the pluton partially surrounding the Oppkuven caldera, contains a good population of euhedral, short zircon crystals with many inclusions of other minerals. Of the six analyses, five are clustered together and give an average $^{206}Pb/^{238}U$ age of 276.6 ± 0.3 Ma. One is older at 279 Ma, most likely due to an inherited component.

5.2.5. Øyangen caldera

The syenite sample representing the ring dyke (KS 23) contained an abundant population of mostly equant, euhedral crystals. The data show some dispersion with two analyses yielding slightly older ages than the main group, possibly indicating some inheritance. The main group of seven data points yields an average $^{206}Pb/^{238}U$ age of 272.3 ± 0.5 Ma (Table 1; Fig. 5).

In contrast to the ring dyke, a syenite from the central complex (KS28) had a scarce zircon population, mostly anhedral and short-prismatic with few euhedral to subhedral ones. Three of the zircon analyses provide coherent results defining an average $^{206}Pb/^{238}U$ age of 272.7 ± 0.5 Ma. Two single grains, richer in U, are instead much younger, likely due to Pb loss.

The ignimbrite (Ø5077) had abundant zircon, mostly euhedral and short- prismatic with many inclusions of other minerals. Cores were not visible, but the data show a spread along the Concordia curve between 276 and 272 Ma. Given the good quality of the analyzed material the spread is attributed to the presence of older inherited zircon. The youngest analysis of euhedral equant grains with a $^{206}Pb/^{238}U$ age of 272.9 ± 0.6 Ma is interpreted as approaching most closely the age of the rhyolite, which is consistent with the other ages obtained for rocks of this caldera.

Sample Ø5070, a rhyolite tuff from the Øyangen caldera, contained a fair amount of zircon, but most of them were highly subrounded with just few euhedral crystals. Three of the latter were analyzed (Table 1) yielding discordant data that indicate Archean, Mesoproterozoic and Neoproterozoic provenances, respectively. Hence the zircon population in the tuff is essentially entirely of detrital origin.

5.3. Late intrusions

5.3.1. Tverrsjøen kjelsåsite pluton

Zircon in kjelsåsite sample N5103 consists mostly of large subequant fragments, rarely showing a crystal face. There is also some baddeleyite. Four zircon analyses overlap on concordia with an average $^{206}Pb/^{238}U$ age of 265.4 ± 0.6 Ma (Table 1, Fig. 6).

5.3.2. Blindern rhomb porphyry-like dyke

The population in the dyke comprises mainly short prismatic to equant crystals. Five analyses yield an average $^{206}Pb/^{238}U$ age of 262.3 ± 0.5 Ma (Table 1, Fig. 6).

6. Discussion

6.1. U-Pb systematics and limitations

A major challenge, complicating the attempts to establish a precise chronostratigraphy for the rhomb porphyry sequence, is the general scarcity or absence of datable zircon in these flows. For example, the initial examination of a thin section of sample KS9 by SEM revealed the presence of several zircon crystals, but they were all smaller than 10 μm, and after mineral separation only one zircon prism large enough to be analyzed could be recovered. Similarly, baddeleyite is found in several of the rhomb porphyry samples, but always as small and thin crystals unsuitable for accurate dating. The scarcity and small size of zircon or baddeleyite is due to the high solubility of Zr in the alkaline melts (Table 2), which prevents their precipitation until late in the crystallization process. High contents of F (0.25 to 0.5%, Larsen et al., 2008) further contribute to increase the Zr solubility. By contrast, there is an opposite effect in larvikites, the plutonic equivalents of the rhomb porphyries, which have an abundance of large zircon (and in part baddeleyite) thanks to the high Zr content and the complete crystallization of the magma.

The second, but related, problem is that the extracted zircon grains tend to be of moderate to low quality for U-Pb dating. They are partially metamict and often skeletal, and tend to disaggregate during chemical abrasion. In several samples the alternative use of air abrasion actually produced better results. For baddeleyite, because of the small and thin geometry of the recovered grains, it was mostly not possible to apply air abrasion and remove the outer parts. And, unfortunately, chemical abrasion does not function with baddeleyite, as demonstrated by Rioux et al. (2010). Some of the Pb (and intermediate Rn) produced near the surface of the grains is lost (by diffusion or leaching) and given the high surface to volume ratio of the mineral the baddeleyite ages are inevitably partially reset, as shown by the several tests done in this study. The baddeleyites analyzed in this study tend to have somewhat higher than normal Th/U (Table 1) suggesting incipient

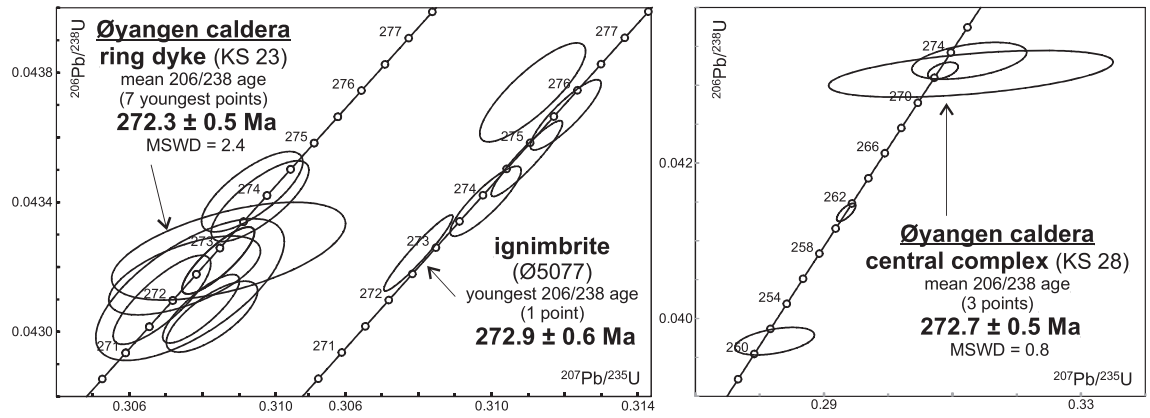

Fig. 5. Concordia plots with U-Pb data of the Øyangen caldera.

transformation to zircon as another potential cause of resetting (e.g. Schaltegger and Davies, 2017), even though no such rims could be seen under the microscope.

The high solubility of Zr in the alkaline magmas (Table 2) prevents the accumulation of inherited zircon, especially in the rhomb porphyry lavas. A much older grain was only found in a sample of RP8, and was likely acquired on surface during the extrusion. The same is likely the case for the older zircon grains present in the rhyolite tuff from the Øyangen caldera (sample Ø5070). The opposite and more difficult question concerns the potential development of zircon as antecrysts in the magma chamber, ahead of extrusion. The evolution of the magmas for rhomb porphyries and larvikites is inferred to have proceeded in stages involving early ponding and differentiation of basaltic magma at the crust mantle boundary before ascent and further differentiation processes (Neumann, 1980). However, the probability that zircon may have crystallized during early magmatic stages is very low. In fact, the rhomb porphyry lavas reach Zr saturation and start precipitating zircon and/or baddeleyite mostly at temperatures between 900 and 850 °C, but for some as low as 670 °C (Table 2; using the model of Gervasoni et al. (2016)), whereas Larsen (1978) calculated magma temperatures of about 1050–1100 °C. Hence, zircon will only start forming at advanced stages of magma crystallization, once the magma temperature decreases and the concentration of Zr (and Tzir) increases in the residual melt (e.g. Siégel et al., 2018). Consequently, some of the scatter in the obtained data, for example for RP6 and 7, is likely related to late stage contamination during emplacement rather than magma chamber processes, with the additional effects of partial Pb loss.

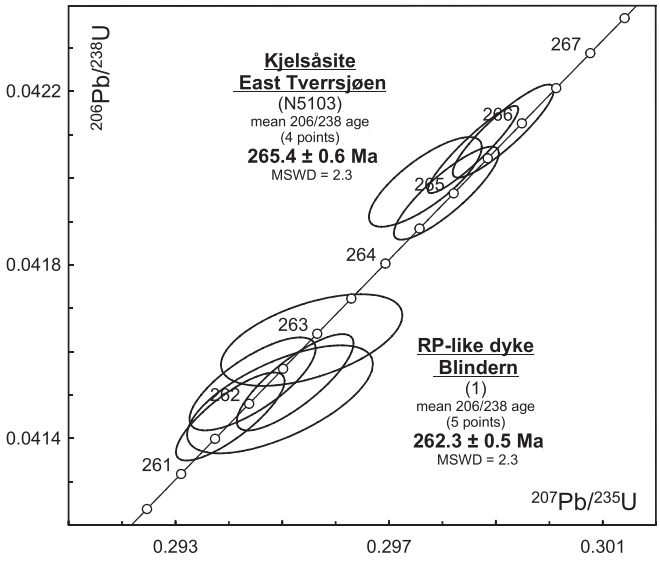

Fig. 6. Concordia plot with U-Pb data of Tverrsjøen kjelsåsite and Blindern RP-like dyke.

6.2. Chronostatigraphy of the Krokskogen region

The new U-Pb data are consistent with, and consolidate the existing age framework established mainly by Rb-Sr (Sundvoll et al., 1990, 1992; Sundvoll and Larsen, 1990, 1993, 1994) and Ar-Ar chronology (Timmerman et al., 2009; Ganerød, pers. comm.), but the higher precision and the inherent information of U-Pb data contributes to an improved temporal resolution. The obtained ages are in agreement with the rhomb porphyry lava stratigraphy and the relative chronology of the other magmatic events in the Krokskogen area as established by field / cross-cutting relations.

6.2.1. Initial rift phase

The zircon U-Pb age of 299.7 ± 0.4 Ma of rhomb porphyry RP1 is the same within error but more precise than the previous Rb-Sr whole rock ages of 292 ± 20 and 291 ± 18 Ma for RP1 at Krokskogen and in Vestfold, respectively, obtained by Sundvoll and Larsen (1990). This age of 299.7 Ma for RP1 corresponds within error to ages of 300.4 ± 0.7 to 299.9 ± 0.9 Ma for the alkalic basalts from the Brunlanes succession in the southern part of the Oslo Graben (Corfu and Dahlgren, 2008b). It is also similar to the 300 ± 1 Ma age of early microsyenitic ("mænaite") sills, which intrude the flanks of the rift. Moreover, because of the stratigraphic superposition, it is a minimum age for the tholeiitic B1 basalts underlying RP1 at Krokskogen, previously constrained by the Rb-Sr WR age of 291 ± 8 Ma (Sundvoll and Larsen, 1990). This diverse, but short-lived, magmatic activity accompanied the late stages of deposition of the Asker Group in the period 303.9 to 299.0 Ma, the terminal Gzhelian stage of the Carboniferous, constrained by fossils of fresh water mussels in the deltaic sequence (Eagar, 1994; Gradstein et al., 2004; Olaussen et al., 1994).

6.2.2. Main rift phase

Following the extrusion of RP1 at 299.7 ± 0.4 Ma, there was a period of 15 m.y. during which flows RP2 to RP5 formed. Due to the lack of zircon in some of the samples we tested for these units, it has not been possible to date these events, and it remains uncertain whether there was a longer magmatic gap after the early activity at 300 Ma, or whether RP2 to RP5 formed at regular intervals during discrete volcanic events. Future work will have to answer this question. But so far we know that the Larvik Plutonic Complex formed between 299 and 292 Ma (Fig. 1; Dahlgren et al., 1996), and alkalic volcanism extruded T1 lava at about 287 Ma (Corfu and Larsen, unpublished data), both of these in the Vestfold Segment. The rhomb porphyry volcanism at Krokskogen was fed from linear sources, and accompanied the development of the rift

Table 2
Zirconium contents and saturation temperatures of typical samples, calculated according to Gervasoni et al. (2016).

Sample ID	Unit	Zr [μg/g]	G	T zir [°C]	Number of zircon grains found
KS-1	B1 basalt	165	2.385	355	–
KS-10	B1 basalt	165	2.383	355	–
KS-18	B2 basalt	408	3.442	605	0
KS-24	caldera basalt	206	2.269	383	–
KS-4	RP1	1250	4.816	886	–
KS-9	**RP1**	**1160**	**4.700**	**867**	**2**
KS-5	RP2	1130	4.495	853	–
KS-6	RP3	1040	4.852	855	–
KS-16	RP3	1140	4.065	829	–
KS-8	RP5	1110	4.591	854	–
KS-2	**RP6**	**836**	**3.986**	**769**	**20 (+b)**
KS-3	RP6	826	3.965	765	0
KS-7	**RP7**	**983**	**5.307**	**867**	**20 (+ b)**
KS-15	RP7	989	5.302	868	–
KS-11	RP8	1130	5.106	882	–
KS-12	RP8	1290	5.196	910	–
KS-19	RP10	567	3.540	671	2
KS-20	RP10	635	3.674	700	0
KS-21	RP11	1030	4.688	845	0
KS-22	**RP11**	**931**	**4.629**	**824**	**>20**
KS-13	RP11	1130	3.325	779	0
KS-14	RP11	1000	5.101	860	0
KS-26	**RP14**	**836**	**4.385**	**792**	**20 (+ b)**
KS-27	RP15	1000	4.253	816	0
KS-25	rhyolite	1030	8.189	980	–
KS-28	**syenite**	**705**	**6.220**	**846**	**>20**
KS-23	**syenite**	**1100**	**6.378**	**931**	**>20**

Notes: samples analyzed in this study (Table 1) are marked in **bold;** Zr = Zr concentration; G = (3 · Al2O3 + SiO2) / (Na2O + K2O + CaO + MgO + FeO) (molar proportions); T zir = zircon saturation temperature; b = baddeleyite; – = sample not processed through mineral separation.

valley and sedimentation of continental character (Olaussen et al., 1994).

Our new data for RP6 flow, RP6–7 conglomerate, and RP7 flow indicate a rapid succession of events at about 285 Ma. Because of pervasive Pb loss, many zircon analyses in these flows are partially reset and do not contribute to improve the precision of the ages. The best estimates of 285.5 ± 0.8 and 284.9 ± 0.5 Ma for RP6 and RP7, respectively, overlap within error. The data for detrital zircons in the intervening conglomerate are broadly consistent with the ages of the two sandwiching flows, but offer no further resolution. The dated (Fjeldstadhytta) conglomerate was deposited along a normal fault, but on both sides of it. Flow RP6 is found immediately on the eastern side of the fault, but only 5 km away from it on its western side, suggesting that the fault is of the same age as RP6. Most (80%) of the clasts are RP5 and the others RP6, with essentially no older clasts.

All these flows were partially eroded, with the local deposition of a younger conglomerate sequence representing alluvial fans and debris flows (Migartjern conglomerate; Olaussen et al., 1994). This unit was then covered by the RP11 flow, which was dated in this study at 280.2 ± 0.5 Ma. A similar age, averaging 279 Ma based on several samples, has also been reported for akerite (quartz monzonite) near Sognsvann (in the southeastern corner of Fig. 2; Borg, 2011). The Siljan-Skrim plutonic complex in the Vestfold segment formed at 282–277 Ma (Pedersen et al., 1995) and trachytic lava (T4) at 282.2 ± 0.4 Ma (Corfu and Dahlgren, 2008a). These events were broadly coeval with the development of early calderas in the Vestfold Graben (Ramnes caldera, Corfu and Larsen, unpublished data) but predated the building phase of central volcanic complexes in the northern sector.

6.2.3. Central volcanoes and Slottet kjelsåsite

The data obtained for the samples representing the Bærum, Oppkuven and Heggelia calderas and the Slottet kjelsåsite coincide, indicating ages between 276.7 and 275.9 Ma (Fig. 4), and thus a relatively short but intense sequence of volcanic and plutonic activities. The Øyangen caldera is instead significantly younger, as indicated by the 272.3 ± 0.5 Ma age of the Ring Dyke and the 272.7 ± 0.5 Ma of the Central Complex. Similar Ar-Ar ages of 273 ± 2.4 Ma and 273 ± 2.8 Ma were reported for kaersutite for syenites of the same caldera (Timmerman et al., 2009). Borg (2011) dated a granitic dyke cutting akerite near Sognsvann at 275 ± 2 Ma.

6.2.4. Batholiths, late plutons and dykes

The last stages of build-up of the rift involved mainly syenitic to granitic plutonism, although some plutonic complexes were in part already built during earlier stages. For example, Haug (2007) reports ages of 287 to 272 Ma for three granitic phases of the Drammen Batholith. In this study we have dated a late intrusions, the Tverrsjøen kjelsåsite (monzodiorite) pluton from the northern part of the Akershus Segment yielding an age of 265.4 ± 0.6 Ma. It predated the 262.3 ± 0.5 Ma Blindern rhomb porphyry-like dyke, and the Tryvann granite (Fig. 2; 259 ± 1 Ma (Corfu and Dahlgren, 2008a), 261 ± 6 Ma (Olsen, 2018)).

6.3. Implications for the development of the Oslo Rift

A number of factors impact the interpretations of the development of the Oslo Rift. These factors are (i) the amount and nature of the magmatic products, (ii) specific mantle domains from which they originate, (iii) processes affecting these domains, (iv) interaction of mantle magmas and heat with the continental crust, (v) degree of extension of crust and subcontinental lithosphere in the region of the rift, (vi) and the relations to large scale tectonic events.

An essential characteristic of the Oslo Rift is its low degree of extension vs. the extensive and multistage magmatic activity (Pallesen, 1994). Important is also the position of the Oslo Rift in the foreland of the Variscan Orogen. As discussed by Olaussen et al. (1994), the northward propagating, east-striking Variscan Tectonic Front in central Europe affected the foreland, activating the Sorgenfrei - Tornquist Zone, and producing extensional stresses north of it, which opened the succession of grabens forming the Oslo Rift. The location of the rift was apparently controlled by a pre-existing lithospheric structure defined by a major down-step and eastward thickening of the lithosphere (Ebbing et al., 2005, 2007; Heeremans et al., 1996). This structure presumably focused the upwelling of the asthenosphere beneath the rift (Pascal et al., 2002, 2004). The origins of the magmas are debated. For example, Pedersen and van der Beek (1994) argued that stretching and melting of a volatile-rich mantle lithosphere were responsible for magmatism in the Oslo Rift, also stressing that the absence of a hotspot track, the initial subsidence, and the relatively low magma production rate did not support a mantle plume explanation. The production rate was estimated on the basis of 8–12 km of mafic magma produced during a period of 40–60 my. Torsvik et al. (2008), however, pointed out that the most significant event of mafic magmatism in the Oslo Rift, southern Sweden, northern Germany and Scotland occurred mainly during a short period at around 297 Ma, the subsequent activity producing mainly felsic magmatic rocks. These authors used a global plate reconstruction to show that at 297 Ma the Skagerrak-Centered Large Igneous Province (SCLIP) was located vertically above the fringes of the African Large Low Shear Velocity Province, the site for almost all Phanerozoic LIPs, thus implying that magmatism was caused by a mantle plume. Based on a study of composite pyroxene phenocrysts in basalts, Neumann (2019) also concludes that a plume was likely responsible for the fresh asthenospheric magma contributions, which formed Cr-poor pyroxene rims around the earlier crystallized Cr-Mg-rich pyroxene cores. The latter are inferred to have formed in magmas derived from depleted, but subsequently metasomatized subcontinental mantle lithosphere.

The new data reported in this paper further stress the importance of the events accompanying the initial burst of magmatism at around

300 Ma. The 299.7 Ma RP1 flows followed extrusion of the tholeiitic B1 basalt in the Akershus segment, and were crudely coeval with increasingly alkalic basalts in the Vestfold Segment, including the melilitic and nephelinitic Brunlanes basalts, and preceding the initial stages of accumulation of the Larvik Batholith. The basalts extruded onto sediments of the Asker Group, hence in an extensional setting. The subsequent 40 m.y. of magmatic activity were characterized by an increasing production of felsic magmas, yet alkalic and basaltic magma were emplaced in volcanoes and as dykes until after 259 Ma, as indicated by the mafic dykes cutting the Tryvann granite (Nilsen, 1992), and also by the young Blindern RP-like dyke dated in this study.

On the large scale of the continent, the burst of the magmatic activity in the Oslo Rift and related areas (Torsvik et al., 2008) corresponded to major late- to post-orogenic granitoid magmatism across the Variscan orogen. It followed the collision of Gondwana and Laurussia, which led to amalgamation and formation of the supercontinent Pangaea and produced far-field stresses in Laurussia (McCann et al., 2006). Gutiérrez-Alonso et al. (2011) propose that orocline formation after collision led to lithospheric thinning, enabling asthenospheric upwelling, mantle melting and subsequent crustal melting. Schaltegger (1997) related the late pulse of magmatism in the Central Variscan belt to collapse (delamination) of the overthickened lithosphere. Clearly, the local interaction of separate tectonic processes affecting the orogen and its boundary zones had ultimately an influence on the events in the Oslo Rift.

7. Conclusions

New U-Pb zircon ages refine the chronostratigraphy of the magmatic evolution in the Krokskogen area of the Oslo Rift. We report a new U-Pb age of 299.7 ± 0.4 Ma for the lowest rhomb porphyry flow RP1, overlapping ages of 285.5 ± 0.8 and 284.9 ± 0.5 Ma for RP6 and RP7, with consistent detrital zircon ages in an intervening conglomerate, indicating rapid sequence of eruptive phases and tectonism at this time, and an age of 280.2 ± 0.5 Ma for RP11. Six samples representing the Bærum, Oppkuven and Heggelia calderas and the Slottet kjelsåsite indicate an intense period of build-up of central volcanoes and plutonism between 276.7 and 275.9 Ma, followed at 273–272 My by the development of the Øyangen caldera. The Tverrsjøen kjelsåsite (monzodiorite) stock from the northern part of the Akershus Segment yields an age of 265.4 ± 0.6 Ma, predating the 262.3 ± 0.5 Ma Blindern rhomb porphyry-like dyke. The new data add evidence for the importance of the magmatic burst at around 300 Ma along the entire Oslo Rift, not just the southern Vestfold Segment and highlight the episodic nature of the subsequent activity until 260 Ma. The new data are not inconsistent with a link between initiation of magmatism and arrival of a mantle plume as proposed by others, but they also emphasize the role for the Oslo Rift activity of the post-Variscan lithospheric stresses in Laurussia. In particular, the fact that both the oldest and youngest rocks dated in this study are rhomb porphyries with similar mineralogical and chemical compositions, and likely similar origin, implies that this magma was produced in the lithosphere almost continuously for the entire period of development of the rift.

Aknowledgments

We thank Gunborg Bye Fjell for her help in mineral separation and SEM examination. Tulio Benitez carried out the initial preparation of part of the samples. Det norske oljeselskap ASA supported the initiation of this project. Morgan Ganerød provided access to geochemical data forthe region. The paper benefitted from constructive reviews by M.J. Timmerman and J. Davies.

Declaration of Competing Interest

There are no conflicts of interest related to this work. All the results have been produced by my co-authors and myself.

References

Borg, G., 2011. Petrology of Akerite (Quartz Monzonite) in the Oslo Rift, SE Norway. MSc thesis. Department of Geosciences, University of Oslo, p. 164.

Brøgger, W., 1933. Om rombeporfyrgangene og de dem ledsagende forkastninger i Oslofeltet. Norges Geol. Unders. Bull. 139, 1–51.

Brøgger, V.C., Schetelig, J., 1917. Geologisk kart Hønefoss, l :100 000. Norges geologiske undersøkelse.

Corfu, F., 2004. U-Pb age, setting and tectonic significance of the anorthosite-mangerite-charnockite-granite suite, Lofoten-Vesterålen, Norway. J. Petrol. 45, 1799–1819.

Corfu, F., Dahlgren, S., 2008a. Chronology of the Oslo Rift: further U-Pb results. 28th Nordic Geological Winter Meeting, Aalborg - Denmark, Jan. 7-10, 2008, p. 20.

Corfu, F., Dahlgren, S., 2008b. Perovskite U-Pb ages and the Pb isotopic composition of alkaline volcanism initiating the Permo-Carboniferous Oslo Rift. Earth Planet. Sci. Lett. 265, 256–269. https://doi.org/10.1016/j.epsl.2007.10.019.

Dahlgren, S., Corfu, F., Heaman, L.M., 1996. U-Pb isotopic time constraints, and Hf and Pb source characteristics of the Larvik plutonic complex, Oslo Paleorift. Geodynamic and Gochemical Implications for the Rift Evolution. V.M. Goldschmidt Conference Abstracts 1, p. 120.

Eagar, R.M.C., 1994. Non-marine bivalve assemblage in the Asker Group, Oslo Graben and its correlation with a late Pennsylvanian assemblage from North America. J. Geol. Soc. Lond. 151, 669–680.

Ebbing, J., Afework, Y., Olesen, O., Nordgulen, Ø., 2005. Is there evidence for magmatic underplating beneath the Oslo Rift? Terra Nova 17, 129–134.

Ebbing, J., Skilbrei, J.R., Olesen, O., 2007. Insights into the magmatic architecture of the Oslo Graben by petrophysically constrained analysis of the gravity and magnetic field. J. Geophys. Res. 112, B04404. https://doi.org/10.1029/2006JB004694.

Gervasoni, F., Klemme, S., Rocha-Júnior, E.R.V., Berndt, J., 2016. Zircon saturation in silicate melts: a new and improved model for aluminous and alkaline melts. Contrib. Mineral. Petrol. 171, 1–12.

Gradstein, F.M., Ogg, J.G., Smith, A.G., et al., 2004. A Geologic Time Scale 2004. Cambridge University Press.

Gutiérrez-Alonso, G., Fernandez-Suarez, J., Jeffries, T.E., Johnston, S.T., Pastor-Galan, D., Murphy, J.B., Franco, M.P., Gonzalo, J.C., 2011. Diachronous post-orogenic magmatism within a developing orocline in Iberia, European Variscides. Tectonics 30, TC5008. https://doi.org/10.1029/2010TC002845.

Harnik, A.B., 1969. Strukturelle Zustände in den Anorthoklasen der Rhombenporphyre des Oslogebietes. Schweizerische Mineralogische und Petrographische Mitteilungen. 49 pp. 509–567.

Haug, L.E., 2007. Mantel og skorpekomponenter i Drammensgranitten, en LAM-ICPMS Lu-Hf isotopstudie av zirkon. MSc thesis. Department of Geosciences, University of Oslo (in Norwegian), p. 105.

Heeremans, M., Larsen, B.T., Stel, H., 1996. Paleostress reconstruction from kinematic indicators in the Oslo Graben, southern Norway. New constraints on the mode of rifting. Tectonophysics 266, 55–79.

Jaffey, A.H., Flynn, K.F., Glendenin, L.E., Bentley, W.C., Essling, A.M., 1971. Precision measurement of half-lives and specific activities of ^{235}U and ^{238}U. Phys. Rev. Sec. Nuclear Phys. 4, 1889–1906.

Krogh, T.E., 1982. Improved accuracy of U-Pb zircon ages by the creation of more concordant systems using an air abrasion technique. Geochim. Cosmochim. Acta 46, 637–649.

Larsen, B.T., 1978. Krokskogen lava area. In: Dons, J.A., Larsen, B.T. (Eds.), The Oslo Paleorift: A Review and Guide to Excursions. Norges geologiske undersøkelse Bulletin. 337, pp. 143–162.

Larsen, B.T., Olaussen, S., Sundvoll, B., Heeremans, M., 2008. The Permo-Carboniferous Oslo Rift through six stages and 65 million years. Episodes 31, 52–58.

Ludwig, K.R., 2009. Isoplot 4.1. A Geochronological Toolkit for Microsoft Excel. Berkeley Geochronology Center Special Publication 4.

Lutro, O., Nordgulen, Ø., 2004. Oslofeltet, berggrunnskart M 1:250 000, Norges geologiske undersøkelse.

Mattinson, J.M., 2005. Zircon U-Pb chemical abrasion ("CA-TIMS") method: combined annealing and multi-step partial dissolution analysis for improved precision and accuracy of zircon ages. Chem. Geol. 220, 47–66. https://doi.org/10.1016/j.chemgeo.2005.03.011.

McCann, T., Pascal, C., Timmerman, M.J., Krzywiec, P., Lopez-Gomez, J., Wetzel, L., Krawczyk, C.M., Rieke, H., Lamarche, J., 2006. Post-Variscan (end Carboniferous-early Permian) basin evolution in Western and Central Europe. In: Gee, D.G., Stephenson, R.A. (Eds.), European Lithosphere Dynamics. Geological Society of London, Memoirs. 32, pp. 355–388.

Neumann, E.-R., 1978. Petrology of the plutonic rocks. In: Dons, J.A., Larsen, B.T. (Eds.), The Oslo Paleorift: A Review and Guide to Excursions. Norges geologiske undersøkelse Bulletin. 337, pp. 25–34.

Neumann, E.-R., 1980. Petrogenesis of the Oslo Region larvikites and associated rocks. J. Petrol. 21, 499–531.

Neumann, E.-R., 2019. Origin and evolution of the early magmatism in the Oslo Rift (Southeast Norway): evidence from multiple generations of clinopyroxene. Lithos 340–341, 139–151. https://doi.org/10.1016/j.lithos.2019.04.025.

Neumann, E.-R., Wilson, M., Heeremans, M., Spencer, E.A., Obst, K., Timmerman, M.J., Kirstein, L., 2004. Carboniferous–Permian rifting and magmatism in southern Scandinavia, the North Sea and northern Germany: A review. In: Wilson, M., Neumann, E.-R., Davies, G.R., Timmerman, M.J., Heeremans, M., Larsen, B.T. (Eds.), Permo-Carboniferous Magmatism and Rifting in Europe. vol. 223, pp. 11–40 Geological Society of London, Special Publications.

Nilsen, O., 1992. Petrology and metallogeny associated with the Tryvann Granite complex, Oslo Region. Norges Geol. Unders. Bull. 423, 1–18.

Oftedahl, C., 1952. Studies on the Igneous Rock Complex of the Oslo Region XII. The Lavas. Norsk Videnskaps-Akademie Skrifter I, Matematisk-Naturvidenskapelige K1asse, No. 3 (64 pp).

Oftedahl, C., 1953. Studies on the Igneous Rock Complex of the Oslo Region XIII. The Cauldrons. Norsk Videnskaps-Akademie Skrifter I, Matematisk-naturvidenskapelige K1asse, No. 3 (108 pp).

Oftedahl, C., 1978. Cauldrons of the Permian Oslo rift. J. Volcanol. Geotherm. Res. 3, 343–371.

Olaussen, S., Larsen, B.T., Steel, R., 1994. The Upper Carboniferous-Permian Oslo Rift; basin fill in relation to tectonic development. Can. Soc. Petrol. Geol. Mem. 17, 175–197.

Olsen, M.T., 2018. Opprinnelsen og alderen til de yngste felsiske plutonene i Oslofeltet. En LAM-MC-ICPMS U-Pb og Lu-Hf isotopstudie av zirkon. Department of Geosciences, University of Oslo (in Norwegian) MSc thesis. (164 pp).

Pallesen, S., 1994. Crustal extension in the Oslo Graben, SE Norway: a method incorporating magmatism and erosion. Tectonophysics 221 (155–117).

Pascal, C., van Wijk, J.W., Cloetingh, S.A.P.L., Davies, G.R., 2002. Effect of lithosphere thickness heterogeneities in controlling rift localization: numerical modeling of the Oslo Graben. Geophys. Res. Lett. 29, 1355. https://doi.org/10.1029/2001GL014354.

Pascal, C., Cloetingh, S.A.P.L., Davies, G.R., 2004. Asymmetric lithosphere as the cause of rifting and magmatism in the Permo- Carboniferous Oslo Graben. In: Wilson, M., Neumann, E.-R., Davies, G.R., Timmerman, M.J., Heeremans, M., Larsen, B.T. (Eds.), Permo-Carboniferous Magmatism and Rifting in Europe. vol. 223. Geological Society of London, Special Publications, pp. 139–156.

Pedersen, T., van der Beek, P., 1994. Extension and magmatism in the Oslo rift, Southeast Norway: no sign of a mantle plume. Earth Planet. Sci. Lett. 123, 317–329.

Pedersen, L.E., Heaman, L.M., Holm, P.M., 1995. Further constraints on the temporal evolution of the Oslo rift from precise U-Pb zircon dating in the Siljan-Skrim area. Lithos 34, 301–315.

Ramberg, I.B., Larsen, B.T., 1978. Tectonomagmatic evolution. In: Dons, J.A., Larsen, B.T. (Eds.), The Oslo Paleorift: A Review and Guide to Excursions. Norges geologiske undersøkelse Bulletin. 337, pp. 55–73.

Rioux, M., Bowring, S., Dudás, F., Hanson, R., 2010. Characterizing the U–Pb systematics of baddeleyite through chemical abrasion: application of multi-step digestion methods to baddeleyite geochronology. Contrib. Mineral. Petrol. 160, 777–801.

Sæther, E., 1962. Studies on the Igneous Rock Complex of the Oslo Region, XVIII. General Investigation of the Igneous Rocks in the Area North of Oslo. Norsk Videnskaps-Akademie Skrifter I, Matematisk-Naturvidenskapelige K1asse, Ny Serie, No. 1 (184 pp).

Schaltegger, U., 1997. Magma pulses in the Central Variscan Belt: Episodic melt generation and emplacement during lithospheric thinning. Terra Nova 9, 242–245.

Schaltegger, U., Davies, J.H.F.L., 2017. Petrochronology of zircon and baddeleyite in igneous Rocks: reconstructing magmatic processes at high temporal resolution. Rev. Mineral. Geochem. 83, 297–328.

Siégel, C., Bryan, S.E., Allen, C.M., Gust, D.A., 2018. Use and abuse of zircon-based thermometers: a critical review and a recommended approach to identify antecrystic zircons. Earth Sci. Rev. 176, 87–116.

Stacey, J.S., Kramers, J.D., 1975. Approximation of terrestrial lead isotope evolution by a two-stage model. Earth Planet. Sci. Lett. 34, 207–226.

Sundvoll, B., Larsen, B.T., 1990. Rb-Sr isotope systematics in the magmatic rocks of the Oslo Rift. Norges Geol. Unders. Bull. 418, 27–46.

Sundvoll, B., Larsen, B.T., 1993. Rb-Sr and Sm-Nd relationship in dyke and sill intrusions in the Oslo Rift and related areas. Norges Geol. Unders. Bull. 425, 23–40.

Sundvoll, B., Larsen, B.T., 1994. Architecture and early evolution of the Oslo Rift. Tectonophysics 240, 173–189.

Sundvoll, B., Neumann, E.-R., Larsen, B.T., Tuen, E., 1990. Age relations among Oslo Rift magmatic rocks: implications for tectonic and magmatic modelling. Tectonophysics 178, 67–87.

Sundvoll, B., Larsen, B.T., Wandås, B., 1992. Early magmatic phase in the Oslo Rift and its related stress regime. Tectonophysics 208, 37–54.

Timmerman, M.J., Heeremans, M., Kirstein, L.A., Larsen, B.T., Spencer-Dunworth, E.A., Sundvoll, B., 2009. Linking changes in tectonic style with magmatism in northern Europe during the late Carboniferous to latest Permian. Tectonophysics 473, 375–390.

Torsvik, T., Smethurst, M., Burke, K., Steinberger, B., 2008. Long term stability in deep mantle structure: evidence from the ~300 Ma Skagerrak-Centered large Igneous Province (the SCLIP). Earth Planet. Sci. Lett. 267, 444–452.